

# Combined fits to the supersymmetric explanation of anomalous lepton- $\gamma$ -missing $E_T$ events

B.C. Allanach<sup>a</sup>, K. Sridhar<sup>b</sup>

<sup>a</sup>*LAPTH, Chemin de Bellevue, B.P. 110, Annecy-le-Vieux 74951, France*

<sup>b</sup>*Department of Theoretical Physics, Tata Institute of Fundamental Research,  
Homi Bhabha Road, Mumbai 400 005, India*

---

## Abstract

The CDF experiment reported a lepton photon missing transverse energy ( $E_T$ ) signal  $3\sigma$  in excess of the Standard Model prediction in Tevatron Run I data. The excess can be explained by the resonant production of a smuon, which subsequently decays to a muon, a photon and a gravitino. Here, we perform combined fits of this model to the CDF  $\gamma l E_T$  excess, the D0 measurement of the same channel and the CDF  $\gamma E_T$  channel. Although the rates of the latter two analyses are in agreement with the Standard Model prediction, our model is in good agreement with these data because their signal to background efficiency is low at the best-fit point. However, they help to constrain the model away from the best fit point.

---

## 1 Introduction

The CDF experiment has recently discovered an anomaly in the production rate of lepton-photon- $E_T$  in  $p\bar{p}$  collisions at  $\sqrt{s} = 1.8$  TeV, using 86.34 pb<sup>-1</sup> of Tevatron 1994-95 data [1]. While the number of events expected from the Standard Model (SM) were  $7.6 \pm 0.7$ , the experimentally measured number corresponded to 16. Moreover, 11 of these events involved muons (with  $4.2 \pm 0.5$  expected) and 5 electrons (with  $3.4 \pm 0.3$  expected).

In earlier papers [2] we suggested that the excess can be simply understood in terms of the minimal supersymmetric standard model (MSSM) which has the following ingredients: (1) the model is  $R$ -parity violating with an  $L$ -violating

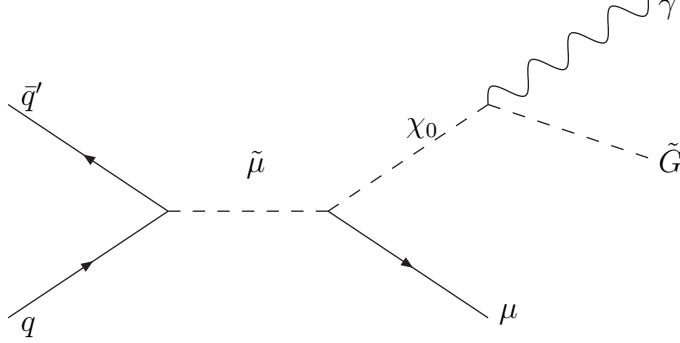


Fig. 1. Feynman diagram of resonant smuon production followed by neutralino decay.

$\lambda'_{211}$  coupling, and (2) the supersymmetric spectrum includes an ultra-light gravitino of mass  $\sim 10^{-3}$  eV. We have demonstrated in our earlier papers [2] that such a model provides a natural explanation of the CDF anomaly and explains not only the excess in the number of  $\mu\gamma\cancel{E}_T$  events but also explains the main features of the kinematic distributions of the excess events. The excess can be explained using a small value of the  $L$ -violating coupling  $\lambda'_{211} \sim 0.01$  because of the resonant production of smuons in the annihilation of an initial-state  $q\bar{q}$  pair. The smuon thus produced decays predominantly into a bino-dominated neutralino and a muon, with the neutralino further decaying into a photon and a gravitino. The production and decay has been shown in the Feynman diagram in Fig. 1. The fact that the excess is seen in final states involving photons emerges very neatly in our model because the decay  $\chi_1^0 \rightarrow \gamma\tilde{G}$  dominates overwhelmingly over other decay modes.

In the current article, we extend the previous studies by including two additional pieces of independent empirical information. We include the D0 Run I measurement [3] of the  $\mu\gamma$  missing  $E_T$  process, as well as  $\gamma$  missing  $E_T$  data coming from CDF in Run I [4]. The empirical background event-rate in the  $\mu\gamma\cancel{E}_T$  channel is quite different in the CDF and D0 cases due to the different cuts employed. Our scenario predicts excesses in each of these channels, and we determine to what extent it is in accord with their measured rates. By performing a combined fit to all three event rates, we constrain the masses of the relevant sparticles in the event, as well as  $\lambda'_{211}$ .

## 2 The model

In order that the cross-section for the production of the smuon resonance is substantial enough to account for the anomalous events, we need the left-

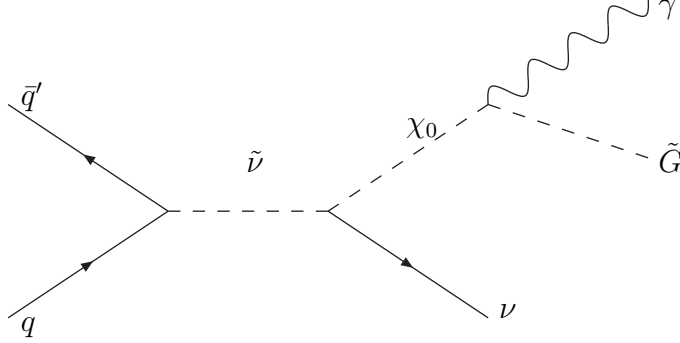


Fig. 2. Feynman diagram of resonant muon sneutrino production followed by neutralino decay, resulting in a  $\gamma\cancel{E}_T$  signature.

handed smuon to be light i.e.  $m_{\tilde{\mu}_L} \sim 150$  GeV. Further, one needs to couple the smuon to valence quarks in the initial state implying that the  $L$ -violating operator that we need is  $L_2 Q_1 \bar{D}_1$  corresponding to the coupling  $\lambda'_{211}$ , which generates the interactions  $\tilde{\mu} u \bar{d}$  and  $\tilde{\nu}_\mu d \bar{d}$  (and charge conjugates), along with other supersymmetrised copies involving squarks. Therefore, the operator we invoke in our model predicts supersymmetric signals in other channels which manifest themselves through the production of either sneutrinos or squarks. In our model, we take the squarks to be heavy and so their effects on experimental observables will be negligible. On the other hand, the spontaneously broken  $SU(2)_L$  symmetry in the MSSM implies that muon sneutrinos have a tree-level mass squared [5]

$$m_{\tilde{\nu}}^2 = m_{\tilde{\mu}_L}^2 - m_\mu^2 + (1 - \sin^2 \theta_w) \cos(2\beta) M_Z^2 \quad \Rightarrow \quad m_{\tilde{\nu}} < m_{\tilde{\mu}_L}, \quad (1)$$

where  $m_\mu$  is the mass of the muon,  $\theta_w$  the Weinberg angle, and  $\tan \beta$  the ratio of the MSSM Higgs vacuum expectation values ( $\cos 2\beta < 0$ ). Since  $m_{\tilde{\nu}} < m_{\tilde{\mu}_L}$  if we assumed that smuons were produced at the Tevatron Run I energy, we should expect that muon sneutrinos could also be produced. The dominant production mechanism is resonant sneutrino production and subsequent decay, as shown in Fig. 2. It results in a  $\gamma\cancel{E}_T$  experimental signature.

The pattern of masses of the super-particles suggested by the CDF  $\mu\gamma\cancel{E}_T$  anomaly is the following: the smuon is around 150 GeV, and the only other light particles are the neutralino (which is typically about 45 GeV lighter than the smuon) and the ultra-light gravitino (which is as light as  $10^{-3}$  eV). We enforce degeneracy between the first two generations in order to avoid flavour changing neutral currents. Other sparticles do not play a role in this analysis, and are set to be arbitrarily heavy. Such a light gravitino materialises naturally in models of gauge-mediated supersymmetry breaking (GMSB)[6]. However, in the minimal version of GMSB models the chargino and the second-lightest

neutralino are not much heavier than the neutralino and this feature of the minimal model is certainly not desirable for our considerations because it leads to large jets+ $\gamma$ + $\cancel{E}_T$  rates which are not seen by experiments<sup>1</sup>. If the minimal versions of GMSB models do not yield the pattern of super-particle masses that we need, then the obvious question to ask is what is the high-energy model that yields this mass spectrum at low energies. It is interesting to note that such a mass spectrum can arise in an alternate model of GMSB which is obtained from compactifying 11-dimensional M-theory on a 7-manifold of G2 holonomy [10]. For the purposes of this paper, however, we simply work with the low-energy model with the mass spectrum described above and do not worry about the high energy completion of this model.

### 3 Simulating the experiments

In our model, we have essentially four free parameters that are relevant to the data we fit: the gravitino mass,  $m_{\tilde{G}}$ , the neutralino mass  $m_{\chi_1^0}$ , the smuon mass,  $M_{\tilde{\mu}}$  and the  $R$ -violating coupling  $\lambda'_{211}$ . However, instead of simultaneously fitting the four parameters using the experimental data, we choose to work with fixed values of two of these parameters close to their best-fit values while performing fits in the two other parameters. For our analysis, we take other parameters like  $\tan\beta = 10$  to be constant. The coupling,  $\lambda'_{211}$ , is constrained from  $R_\pi = \Gamma(\pi \rightarrow e\nu)/(\pi \rightarrow \mu\nu)$  [11] to be  $< 0.059 \times \frac{m_{\tilde{d}_R}}{100 \text{ GeV}}$  [12]. But since the constraint involves a squark mass which is large in our model, it is not very relevant. While the production of the smuon resonance is through the  $R$ -violating mode, to produce the  $l\gamma\cancel{E}_T$  excess we require that its decay goes through the  $R$ -conserving channel to a neutralino and muon final state. The  $R$ -violating decay of the slepton is possible but constrained, in principle, by the Tevatron di-jet data [13] which exclude a  $\sigma.B > 1.3 \times 10^4$  pb at 95% C.L. for a resonance mass of 200 GeV. However, in practice this does not provide a restrictive bound upon our scenario as long as the  $R$ -violating coupling is sufficiently small,  $< \mathcal{O}(1)$ . We also add that the di-jet bound is not restrictive because it suffers from a huge QCD background. By restricting  $\lambda'_{211}$  to be small, we also avoid significant rates for the possible  $R$ -violating decays of  $\chi_1^0 \rightarrow \mu jj$  or  $\chi_1^0 \rightarrow \nu jj$ .

We use the ISASUSY part of the ISAJET7.58 package [14] to generate the spectrum, branching ratios and decays of the sparticles. For an example of parameters, we choose (in the notation used by ref. [14])  $\tan\beta = 10$  and  $A_{t,\tau,b} = 0$ .  $\mu$  together with other flavour diagonal soft supersymmetry breaking parameters

---

<sup>1</sup> This observation has been made earlier in the literature [7] in the context of the GMSB-based explanation [8] of the  $ee\gamma\gamma\cancel{E}_T$  CDF event [9].

$E_T(\gamma)/\text{GeV}$	<60	60-65	65-80	>80
efficiency	40%	47%	51%	54%

Table 1

Photon efficiency in the CDF  $\gamma\cancel{E}_T$  analysis

experiment	luminosity	observed number	background
CDF $l\gamma\cancel{E}_T$	86 pb <sup>-1</sup>	11	4.2 ± 0.5
D0 $\mu\gamma\cancel{E}_T$	73 pb <sup>-1</sup>	58	58 ± 9.75
CDF $\gamma\cancel{E}_T$	86 pb <sup>-1</sup>	11	11 ± 2.2

Table 2

Observed number of events passing cuts in the text and Standard Model backgrounds for the three pieces of data included in the combined fit. The integrated luminosity for each analysis is also listed.

are set to be very large. We emphasise that this is a representative point in the supersymmetric parameter space and not a special choice.

As stated earlier, we present analyses for three sets of data in this paper: the CDF Run I data on  $l\gamma\cancel{E}_T$  [1], the D0 Run I data on  $\mu\gamma\cancel{E}_T$  [3] and the CDF Run I data on  $\gamma\cancel{E}_T$  [4]. We now present our fiducial efficiencies and cuts, which mimic those of the relevant experiments. The CDF experiment detects photons with the constraints that the following pseudo-rapidity regions are excluded:  $|\eta^\gamma| > 1$ ,  $|\eta^\gamma| < 0.05$  and the region  $0.77 < \eta^\gamma < 1.0$ ,  $75^\circ < \phi < 90^\circ$ . For the  $l\gamma\cancel{E}_T$  data, photon detection efficiency within these cuts is  $\eta_\gamma = 81\%$ . Muons have a 60% detection efficiency if  $|\eta_\mu| < 0.6$  or 45% if  $0.6 \leq \eta_\mu \leq 1.1$ . To improve signal to background ratio efficiency, the following cuts are used:  $E_T(\mu) > 25$  GeV,  $E_T(\gamma) > 25$  GeV and  $\cancel{E}_T > 25$  GeV. For the  $\gamma\cancel{E}_T$  analysis, the CDF experiment [4] has chosen the following cuts:  $|\eta^\gamma| \leq 1.0$ ,  $E_T^\gamma > 55$  GeV and  $\cancel{E}_T > 45$  GeV. The cut on the photon  $E_T$  is chosen to be as large as 55 GeV so as to beat down the background due to cosmic rays. Photon fiducial efficiencies are shown in table 1, and were obtained from ref. [4]

In contrast, in order to simulate the D0 experiment, we specify  $|\eta_\mu| \leq 1.0$ ,  $|\eta_\gamma| \leq 1.1$  or  $1.5 \leq |\eta_\gamma| \leq 2.5$ . We use the same cuts as D0:  $p_T^\mu > 15$  GeV,  $p_T^\gamma > 10$  GeV on the muon and photon  $p_T$  respectively. Also,  $\cancel{E}_T \geq 15$  GeV,  $\Delta R(\mu\gamma) \geq 0.7$  and  $M_T(\mu\cancel{E}_T) \geq 30$  GeV. Here,  $\Delta R(\mu\gamma)$  is the distance between the photon and muon in pseudo-rapidity ( $\eta$ ) and transverse angle ( $\phi$ ) space.  $M_T^2 \equiv E_T^2 - p_T^2$  is the transverse mass. Within these cuts, we have fiducial efficiencies of 71.1%, 50.1% and 51.0% for the trigger, muon and photon respectively. These cuts have been optimised by D0 with a view to studying the effects of anomalous gauge boson couplings on this final state. Unfortunately, the signal to background ratio for our model in the D0 analysis is far from optimal for the signal that we propose to study.

The observed number of events in the different analyses, and their Standard Model backgrounds (taken from the experimental papers [1,3,4]) are shown in Table 2.

We now simulate the signal events for the processes in Figs. 1,2. We use HERWIG6.4 [15] including parton showering (but not including jet isolation cuts) to calculate cross-sections for single slepton production.

#### 4 Combined fits

For each of the three data listed in Table 2, we can define a log likelihood defined by the Poissonian log-likelihood for  $n_o$  observed events,  $n_s$  expected signal events (for fixed values of SUSY breaking parameters), convoluted with a Gaussian probability distribution of the number of expected Standard Model background events  $n_{SM}$  and its uncertainty  $\sigma_{SM}$ :

$$\ln \mathcal{L}(n_s) \equiv \frac{1}{\sqrt{2\pi}\sigma_{SM}} \int_0^\infty e^{-\frac{(n-n_{SM})^2}{2\sigma_{SM}^2}} (n_o \ln(n+n_s) - (n+n_s) - \ln n_o) dn. \quad (2)$$

This is a good approximation provided  $n_{SM}$  is several times  $\sigma_{SM}$  above zero, as is the case here.  $\ln(\mathcal{L}(n_s)/\mathcal{L}(0))$  is then the (signal+background) to background likelihood ratio for a given analysis. We can form the total fit likelihood ratio  $\ln \mathcal{L}^{tot}$  by adding the likelihood ratio from each of the three analyses in Table 2. We will always consider two relevant parameters to be fixed and fit the model to the other two. The best-fit point in parameter space corresponds to the maximum value of the likelihood ratio and is found by using MINUIT [16].  $-2 \ln \mathcal{L}_{max}^{tot}$  corresponds to the equivalent number of  $\chi^2$  (Standard Model) -  $\chi^2$  (best-fit)  $\equiv \Delta\chi^2$ . We have one degree of freedom, and therefore the 90% and 95% confidence level (*C.L.*) limits on parameters then lead to [16]  $\ln \mathcal{L}_{max}^{tot} - \ln \mathcal{L}^{tot} = 1.35, 1.92$  respectively in the fit. We will constrain  $M_{\chi_1^0} > 100$  GeV, as implied by  $\gamma\gamma\cancel{E}_T$  LEP2 data [17]. We now discuss the results of combined fits for various hyper planes of parameter space.

Fig. 3 displays the 90 and 95% *C.L.* fit regions as the area between the solid lines in the  $\lambda'_{211}, M_{\chi_1^0}$  plane.  $\Delta m \equiv M_{\tilde{\mu}} - M_{\chi_1^0}$  has been kept fixed at 45 GeV in order to keep the decay mode  $\tilde{\mu} \rightarrow \mu\chi_1^0$  open and  $m_{\tilde{G}} = 10^{-3}$  eV. A significant amount of parameter space fits the combined data, with ranges  $\lambda'_{211} > 0.001$ . Increasing  $M_{\chi_1^0}$  produces a lower cross-section because of kinematical suppression, but this effect can be compensated by raising  $\lambda'_{211}$ , thus increasing the production rate. The best-fit point is  $\lambda'_{211} = 0.11$ ,  $M_{\chi_1^0} = 100$  GeV, with  $\Delta\chi^2 = 6.90$ . Fig. 3a shows that we expect between 3-8 signal events in the CDF  $l\gamma\cancel{E}_T$  channel. This data dominates the fit because backgrounds (and

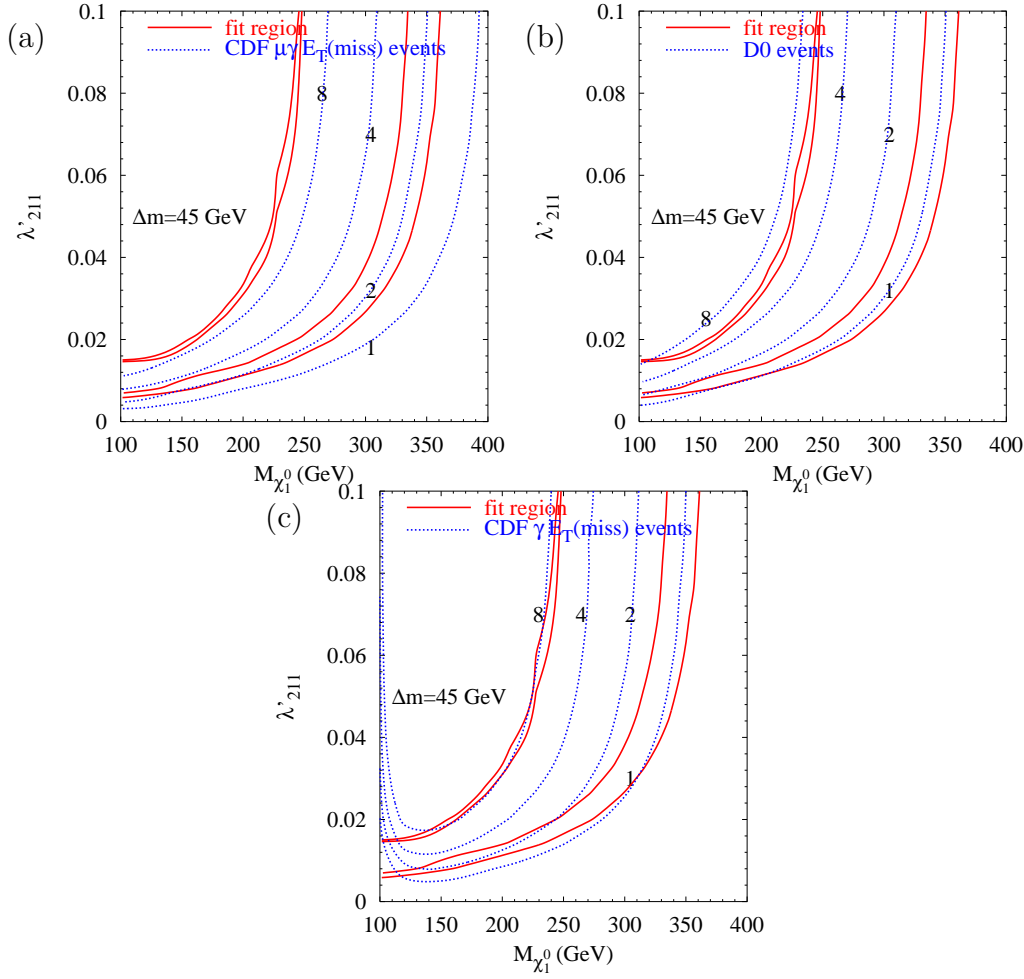


Fig. 3. Predicted number of excess events in (a) CDF  $l\gamma\cancel{E}_T$ , (b) D0  $l\gamma\cancel{E}_T$ , and (c) CDF  $\gamma\cancel{E}_T$  channels in the  $\lambda'_{211}$ -neutralino mass plane for  $\tan\beta = 10$ ,  $\Delta m = 45$  GeV and  $m_{\tilde{G}} = 10^{-3}$ . Labelled contours of equal numbers of signal events are shown as dashed curves. The 90% *C.L.* and 95% *C.L.* combined-fit regions are between the inner and outer pair of solid lines respectively.

their uncertainties) are larger in the other analyses. 1.5-6 events are expected at D0, and between 1.5 and 8 signal events were predicted for the CDF  $\gamma\cancel{E}_T$  signature, depending on the parameters.

Fig. 4 displays the 90 and 95% *C.L.* fit regions as the area to the left-hand side of the solid lines in the  $\log(m_{\tilde{G}}), M_{\chi_1^0}$  plane. Here, we use the default values  $\lambda'_{211} = 0.01$ ,  $\Delta m = 45$  GeV. It is clear from the fit regions that the data prefer lower values of the neutralino mass. The best-fit point is:  $M_{\chi_1^0} = 100$  GeV,  $m_{\tilde{G}} = 10^{-3.0}$  eV,  $\Delta\chi^2 = 6.76$ . The figure illustrates that if  $m_{\tilde{G}} > 0.1$  eV, the branching ratio of  $\chi_1^0 \rightarrow \tilde{G}\gamma$  becomes tiny, decreasing the cross-section for the CDF  $l\gamma\cancel{E}_T$  signal, which dominates the fit. When  $m_{\tilde{G}}$  is below  $10^{-5}$  eV,  $\tilde{\mu} \rightarrow \mu\tilde{G}$  decays dominate, again decreasing the CDF  $\mu\gamma\cancel{E}_T$  signal. 2-6 CDF  $l\gamma\cancel{E}_T$  excess events, 2-4 D0 excess events and 0-3  $\gamma\cancel{E}_T$  CDF excess events are expected, shown by the dashed contours within the 90% *C.L.* regions of

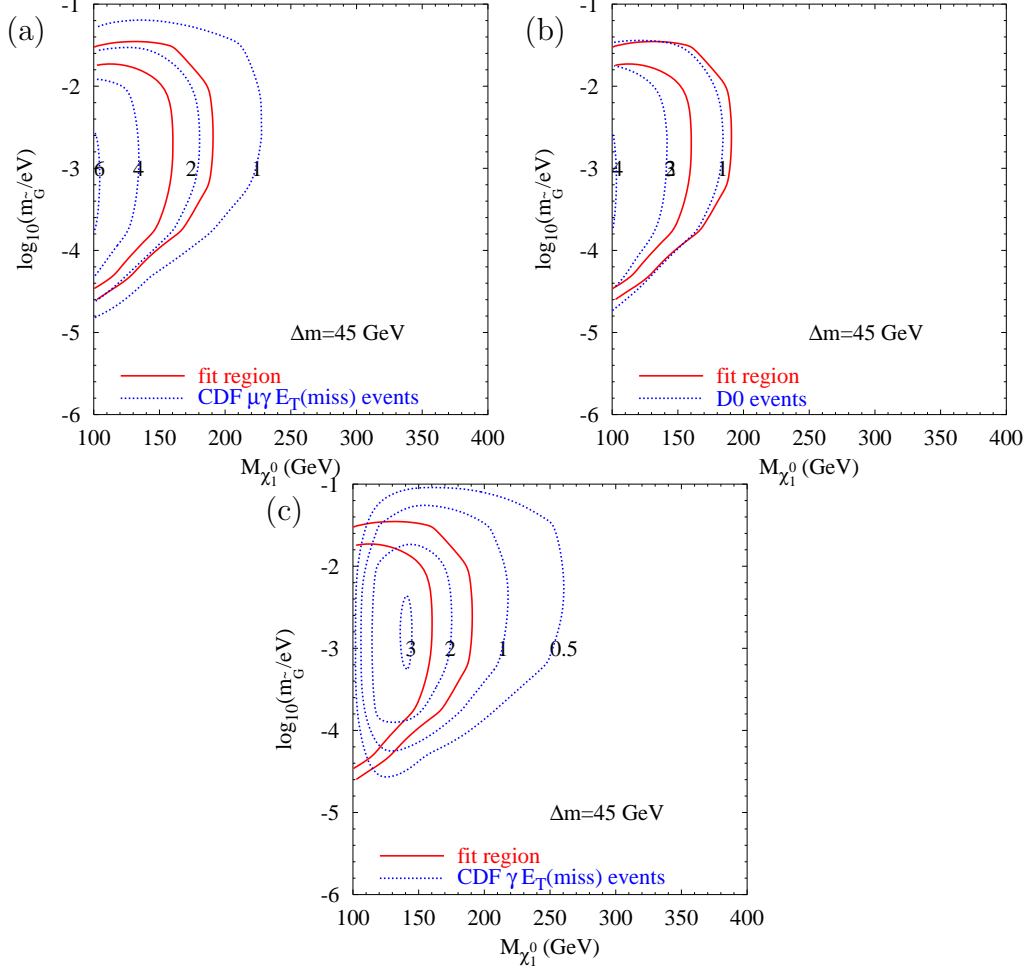


Fig. 4. Predicted number of excess events in (a) CDF  $l\gamma\cancel{E}_T$ , (b) D0  $l\gamma\cancel{E}_T$ , and (c) CDF  $\gamma\cancel{E}_T$  channels in the gravitino mass-neutralino mass plane, for  $\tan\beta = 10$ ,  $\Delta m = 45$  GeV and  $\lambda'_{211} = 0.01$ . Labelled contours of equal numbers of signal events are shown as dashed curves. The 90% *C.L.* and 95% *C.L.* combined-fit regions are to the left of the inner and outer solid lines respectively.

Figs. 4(a-c).

Fig. 5 displays the 90 and 95% *C.L.* fit regions as the area between the solid lines in the  $\lambda'_{211}, M_{\tilde{\mu}}$  plane. Here we have chosen default values of  $m_{\tilde{G}} = 10^{-3}$  eV and  $M_{\chi_1^0} = 100$  GeV. A significant amount of parameter space fits the combined data. The best-fit point is  $\lambda'_{211} = 0.114$ ,  $M_{\tilde{\mu}} = 154$  GeV, with  $\Delta\chi^2 = 6.90$ . Fig. 5a shows that we expect between 1-12 signal events in the CDF  $l\gamma\cancel{E}_T$  channel. 1-8 events are expected at D0, and up to 4 signal events were predicted for the CDF  $\gamma\cancel{E}_T$  signature, depending on the parameters.

Fig. 6 displays the 90 and 95% *C.L.* fit regions as the area enclosed by the solid lines in the  $m_{\tilde{G}}, M_{\tilde{\mu}}$  plane. Here we have chosen default values of  $\lambda'_{211} = 0.01$  and  $M_{\chi_1^0} = 100$  GeV. The ranges  $M_{\tilde{\mu}} = 130 - 230$  GeV,  $m_{\tilde{G}} = 10^{-4.5} - 10^{-1.5}$  eV provide a reasonable combined fit. The best-fit point is  $m_{\tilde{G}} = 10^{-3.1}$  eV,



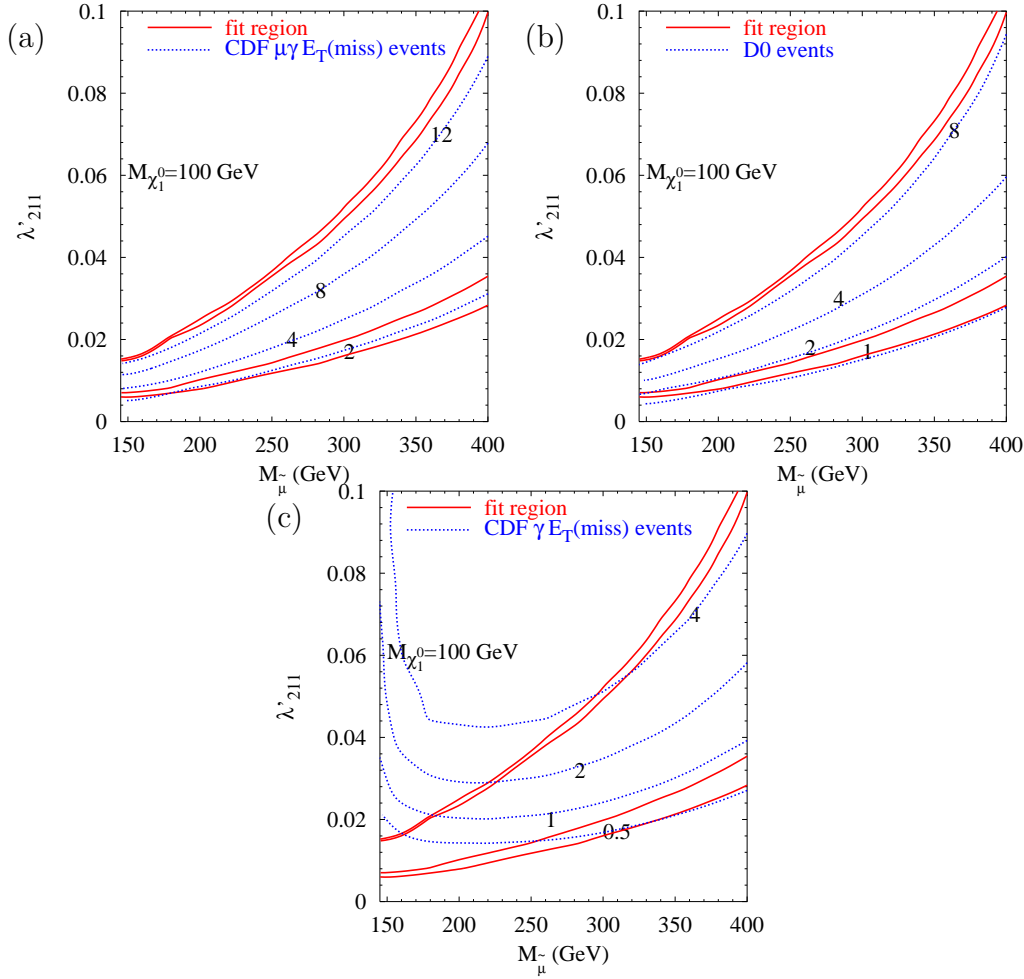


Fig. 5. Predicted number of excess events in (a) CDF  $l\gamma\cancel{E}_T$ , (b) D0  $l\gamma\cancel{E}_T$ , and (c) CDF  $\gamma\cancel{E}_T$  channels in the  $\lambda'_{211}$ -smuon mass plane, for  $\tan\beta = 10$ ,  $m_{\tilde{G}} = 10^{-3}$  eV and  $M_{\chi_1^0} = 100$  GeV. Labelled contours of equal numbers of signal events are shown as dashed curves. The 90% *C.L.* and 95% *C.L.* combined-fit region is between the inner and outer pair of solid lines respectively.

$M_{\tilde{\mu}} = 142$  GeV, with  $\Delta\chi^2 = 6.76$ . Fig. 6a shows that we expect between 1-6 signal events in the CDF  $l\gamma\cancel{E}_T$  channel. 0-4 events are expected at D0, and up to 0.2 signal events were predicted for the CDF  $\gamma\cancel{E}_T$  signature, depending on the parameters.

## 5 Conclusions

We have provided combined fits for a supersymmetric model that explains the  $l\gamma\cancel{E}_T$  CDF Run I excess in events, which was at the  $2.7\sigma$  level [1]. We have used the Run I  $\gamma\cancel{E}_T$  data recently presented by CDF, as well as anomalous trilinear gauge boson coupling data from D0. Constraints upon various hyper planes in the gravitino, smuon, neutralino and R-parity violating coupling space have

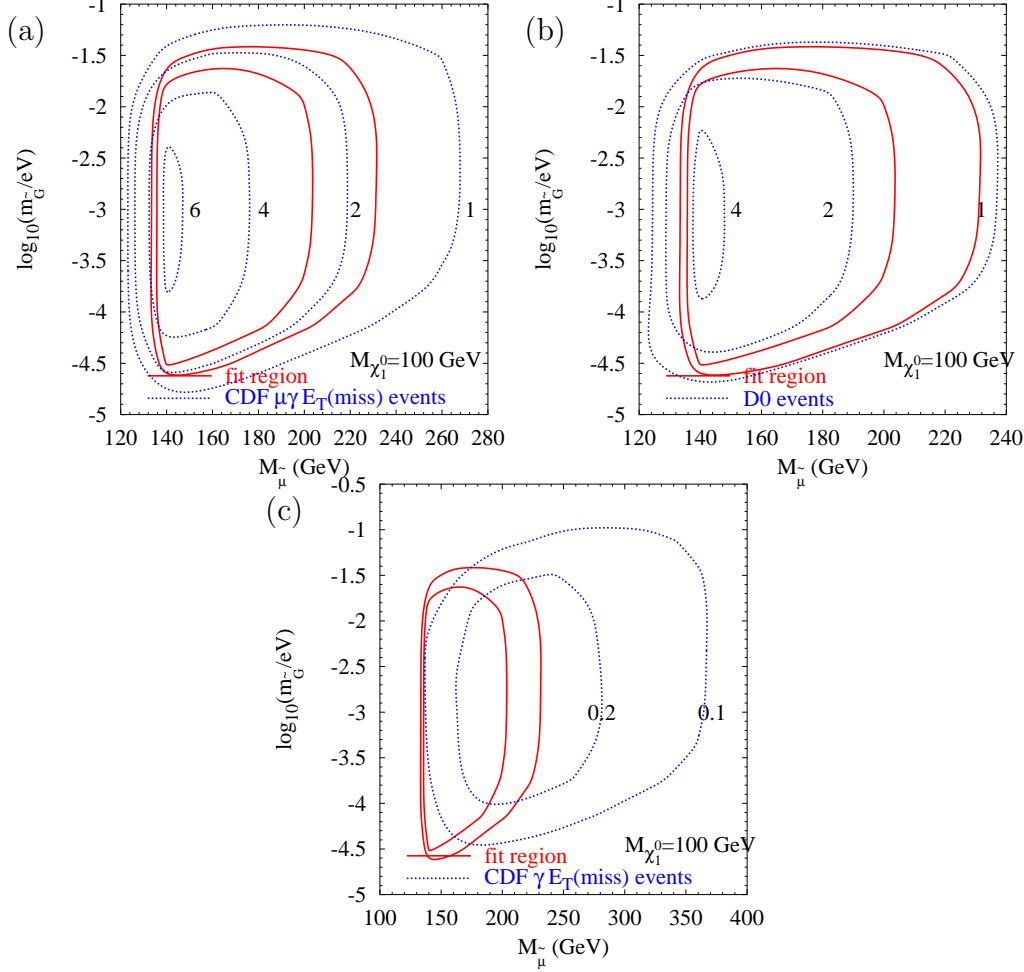


Fig. 6. Predicted number of excess events in (a) CDF  $l\gamma E_T$ , (b) D0  $l\gamma E_T$ , and (c) CDF  $\gamma E_T$  channels in the gravitino mass-smuon mass plane, for  $\tan\beta = 10$ ,  $M_{\chi_1^0} = 100 \text{ GeV}$  and  $\lambda'_{211} = 0.01$ . Labelled contours of equal numbers of signal events are shown as dashed curves. The 90% *C.L.* and 95% *C.L.* combined-fit regions are depicted by solid lines.

been displayed. In totality, the signal rates predicted by our model for the three analyses fit the data well, best fit points corresponding to a  $\Delta\chi^2 = 6.9$  fit compared to the Standard Model, for one degree of freedom.

Unfortunately, background rates in the D0 anomalous trilinear gauge boson coupling data are too high for it to be very sensitive to the predicted signal rate. We note, however, that another analysis on existing D0 Run I data with cuts optimised to test a  $\mu\gamma E_T$  excess would provide a good test of our scenario.

The CDF  $\gamma E_T$  channel suffers from a high  $E_T(\gamma) > 55$  cut because of cosmic backgrounds, which unfortunately also cuts most of the signal. It was shown in ref. [2], that if the cut could be reduced to 25 GeV, a signal rate of several times that in the CDF  $l\gamma E_T$  channel is possible. This is an important observation for Run II, where cosmic backgrounds could be cut by additional timing

information in the detector. We look forward to the analysis of Run II data, which will be the final arbiter on  $l\gamma\cancel{E}_T$  excess, as well as on our scenario.

## Acknowledgements

We would like to thank J. Berryhill, H.J. Frisch, S. Hagopian, D. Toback and D. Wood for help and advice regarding experimental analyses and data. We would also like to thank CERN, where much of this work was carried out.

## References

- [1] D. Acosta et al, Phys. Rev. D66 (2002) 012004, hep-ex/0110015; D. Acosta et al, Phys. Rev. Lett. 89 (2002) 041802, hep-ex/0202044.
- [2] B.C. Allanach, S. Lola and K. Sridhar, Phys. Rev. Lett. 89 (2002) 011801, hep-ph/0111014; B.C. Allanach, S. Lola and K. Sridhar, JHEP 0204 (2002) 002, hep-ph/0112321.
- [3] S. Abachi et al, Phys. Rev. Lett. 78 (1997) 3634, hep-ex/9612002.
- [4] D. Acosta et al, hep-ex/0205057; T. Fahland, Ph. D. thesis (1997) Brown University, can be viewed at URL [http://www-d0.fnal.gov/results/publications\\_talks/thesis/fahland/thesis.ps](http://www-d0.fnal.gov/results/publications_talks/thesis/fahland/thesis.ps)
- [5] B.C. Allanach, Comput. Phys. Comm. 143 (2002) 305, hep-ph/0104145.
- [6] G. Giudice and R. Rattazzi, Phys. Rept. 322 (1999) 419 and references therein.
- [7] H. Baer, M. Brhlik, C. Chen and X. Tata, Phys. Rev. D55 (1997) 4463.
- [8] S. Ambrosanio, G. L. Kane, G. D. Kribs, S. P. Martin, and S. Mrenna, Phys. Rev. Lett. 76 (1996) 3498; G. L. Kane and S. Mrenna, Phys. Rev. Lett. 77 (1996) 3502; S. Ambrosanio, G. L. Kane, G. D. Kribs, S. P. Martin, and S. Mrenna, Phys. Rev. D55 (1997) 1372.
- [9] F. Abe et al, Phys. Rev. D59 (1999) 092002.
- [10] E. Witten, hep-ph/0201018 and talk at SUSY 2002, can be viewed at URL <http://www.desy.de/~susy02/pl.6/witten.pdf>
- [11] V. Barger, G. F. Giudice and T. Han, Phys. Rev. D 40 (1989) 2987.
- [12] B. C. Allanach, A. Dedes, and H. K. Dreiner, Phys. Rev. D60, 075014 (1999), hep-ph/9906209; H. Dreiner, ‘Perspectives on Supersymmetry’, Ed. by G.L. Kane, World Scientific.
- [13] F. Abe et al, Phys. Rev. D55 (1997) 5263.

- [14] F. E. Paige, S. D. Protopescu, H. Baer and X. Tata, hep-ph/9810440.
- [15] G. Corcella et al, hep-ph/0201201; G. Marchesini, B. R. Webber, G. Abbiendi, I. G. Knowles, M. H. Seymour and L. Stanco, JHEP 01 (2001) 010 hep-ph/0011363; *ibid.* hep-ph/0107071. “HERWIG: A Monte Carlo event generator for simulating hadron emission reactions with interfering gluons. Version 5.1 - April 1991”, Comput. Phys. Commun. 67 (1992) 465.
- [16] F. James and M. Roos, Comput. Phys. Commun. 10 (1975) 343.
- [17] LEPSUSYWG, ALEPH, DELPHI, L3 and OPAL experiments, note LEPSUSYWG/02-07.1  
<http://lepsusy.web.cern.ch/lepsusy/Welcome.html>